Author for correspondence:
Kaimin Chen
e-mail: kmchen@sues.edu.cn

Synthesis of poly(acrylic acid) coated magnetic nanospheres via a multiple polymerization route

Kai Li[1], Kaimin Chen[1], Qiaoling Wang[1], Ying Zhang[2] and Wenjun Gan[1]

[1]College of Chemistry and Chemical Engineering, Shanghai University of Engineering Science, Shanghai 201620, People's Republic of China
[2]State Key Laboratory of Chemical Engineering, School of Chemical Engineering, East China University of Science and Technology, Shanghai 200237, People's Republic of China

KC, 0000-0002-1238-7340

Magnetic nanospheres are versatile candidates for both fundamental and practical applications. Before they are applied in more complicated fields, their surface must be modified by several functionalities. However, the surface modification can be affected by the magnetic nanoparticles (MNP) embedded in the polymer matrix. Herein, the synthesis of poly(acrylic acid) coated magnetic nanospheres via a multiple polymerization route is described. During the synthesis process, seed emulsion polymerization was applied to redistribute the MNP in the polymer matrix, and the relationship between the structure of magnetic nanospheres and the thickness of the grafted poly(acrylic acid) layer was investigated. The development of size, morphology and magnetic properties of the nanospheres were characterized by transmission electron microscopy, dynamic light scattering, thermogravimetric analysis, X-ray diffraction and vibrating sample magnetometry. This work would pave the way to design and preparation of new structure of functional magnetic nanospheres with precise surface modification.

1. Introduction

Magnetic polymer nanospheres combine the special properties of inorganic magnetic nanoparticles (MNP) and functional polymeric materials, which have many potential applications [1,2] in the treatment of waste oil pollution in the ocean [3], drug delivery [4–6], separation and purification of biological materials [7], contrast agents [8], adsorption of heavy metal ions [9], and hyperthermia [10]. Among these applications, the magnetic
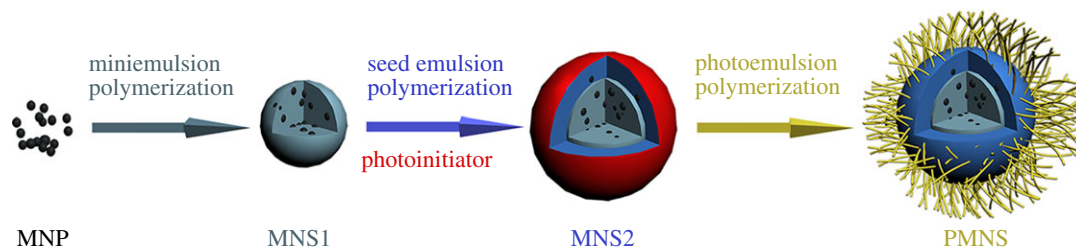
Scheme 1. Schematic illustration of the preparation of the poly(acrylic acid) coated magnetic nanospheres (PMNS).

polymer nanospheres are mainly used as a carrier to bind materials such as biomolecules and can be easily manipulated by an external magnetic field. For example, Oster *et al.* used poly(vinyl alcohol)-based magnetic beads to separate genomic DNA and purify sequence specific nucleic acid [11]. Nishio *et al.* synthesized magnetic nano-carriers with poly(glycidyl methacrylate) on the surface, which could immobilize many types of drugs and could be used in separation of proteins by affinity purification [12]. Therefore, the functional group modification on the surface of the magnetic nanospheres greatly enhances their performance in a variety of applications.

Researchers have reported various functional groups on magnetic polymer nanospheres, such as hydroxyl groups [13], amino groups [14–16], thiol groups [17], epoxy groups [18,19] and carboxyl groups. Among them, there are many interesting works on the study of carboxyl groups [3,20–22]. Carboxyl groups can be used as a carrier for catalysts [23,24], agent for adsorption of proteins [25,26], and template for the synthesis of metal nanoparticles [27,28]. Carboxyl groups also provide high stability in water and can be stored for a long time [22]. However, it was found that the surface modification by functional groups was greatly affected by the employed synthesis route in the preparation of magnetic nanospheres.

In previous studies, researchers have been working on the development of various polymerization methods, such as suspension polymerization [29,30], precipitation polymerization [31], emulsion polymerization [32], miniemulsion polymerization [33–37], soap-free emulsion polymerization [38], to control the morphology of magnetic polymer nanospheres. In these studies, miniemulsion polymerization is considered to be the most effective way to encapsulate inorganic nanoparticles [35]. In order to further improve the encapsulation of MNP, some researchers have adopted the method of multi-step polymerization. They either synthesized magnetic beads firstly and then immobilized the carboxyl-containing nanoparticles onto the magnetic bead surface by self-assembly [39,40] or used more complicated methods to improve the morphology of magnetic polymer nanospheres [19,41]. However, there is still a lack of a cost-effective way to balance the surface modification of nanospheres and MNP existing in the polymer matrix. Therefore, we provide an alternative way to prepare functional magnetic nanospheres.

In our work, a multiple polymerization route was used to prepare poly(acrylic acid) (PAA) coated magnetic nanospheres (PMNS). A strategy combining three polymerization methods including miniemulsion polymerization, seed emulsion polymerization and photoemulsion polymerization was used here (scheme 1). Especially, seed emulsion polymerization was applied to control the MNP distribution in polystyrene. At the same time, the effect of aggregation state of MNP in magnetic nanospheres on surface functionalization was also studied.

2. Material and methods

2.1. Chemicals

Iron acetylacetonate (Fe(acac)$_3$), oleic acid (OA), oleylamine, absolute ethanol, biphenyl ether, *n*-hexane, sodium dodecylsulfate (SDS), hexadecane (HD), and methacryloyl chloride (MC) were purchased from Adamas Reagent Co., Ltd. 2-Hydroxy-4′-hydroxyethoxy-2-methylpropiophenone (HMP) (Irgacure 2959) was purchased from SANN Chemical Technology Shanghai Co., Ltd. 1,2-Dodecanediol was bought from Tokyo Chemical Industry Co., Ltd. Potassium persulfate (KPS) was obtained from Shanghai Lingfeng Chemical Regent Co., Ltd. Styrene (St) and acrylic acid (AA) (from Shanghai Titan Scientific Co., Ltd) were distilled under reduced pressure and placed in a 4°C refrigerator for later use. The

photoinitiator   2-[*p*-(2-hydroxy-2-methylpropiophenone)]-ethylene-glycol-methacrylate   (HMEM)   was prepared according to previous work [20].

2.2. Preparation of magnetic nanoparticles

MNP were prepared by a pyrolysis process [42]: Fe(acac)$_3$ (1.42 g), biphenyl ether (40 ml), 1,2-dodecanediol (4.05 g), OA (3.39 g), and oleylamine (3.21 g) were mixed in a 250 ml three-necked flask. Under nitrogen atmosphere and magnetic stirring, the temperature was raised to 200°C and kept for 2 h. Then the temperature was raised to 260°C, refluxed for 2 h and cooled down to room temperature. An amount of 80 ml of absolute ethanol was added to the black mixture and centrifuged at 10 000 rpm for 20 min to obtain a black precipitate. To purify MNP, the black sediment was redispersed in 10 ml of *n*-hexane (0.1 ml of OA and 0.1 ml of oleylamine were added simultaneously) and the residue was removed by centrifugation at 6000 rpm for 10 min. Finally, the MNP were obtained through re-precipitation with ethanol, and were redispersed in *n*-hexane (20 wt%), kept at a low temperature (4°C) for later use.

2.3. Preparation of seed magnetic nanospheres

An amount of 0.01 g of SDS was completely dissolved in 10 g of deionized water. A mixture of 0.05 g of HD, 1 g of styrene and 0.05 g magnetic fluid (20 wt%) was made in a test tube, followed by ultrasonication with a frequency of 53 kHz and a power of 350 W for 15 min. The sonicated mixture was then placed in a 30 ml sample vial and mixed with SDS solution and then homogenized (Ultrasonic Cell Shredder from Ningbo Xinzhi Biotechnology Co., Ltd) for 10 min to obtain a pre-emulsion. An amount of 5 ml of KPS solution (0.002 g ml^{-1}) was mixed with the pre-emulsion and added to a 100 ml three-necked flask. The miniemulsion polymerization was carried out under nitrogen protection at 80°C with mechanical stirring of 300 rpm for 20 h. The emulsion was then subjected to dialysis treatment for further use. These magnetic nanospheres synthesized by miniemulsion polymerization are denoted as seed magnetic nanospheres (MNS1).

## 2.4. Preparation of magnetic nanospheres coated by photoinitiator

A mixture of SDS solution (0.002 g solid) and KPS solution (0.005 g solid) was added into a three-necked flask. A suitable amount of MNS1 emulsion was then added as a seed emulsion, and extra deionized water was added to make the total amount of water 20 g. The mixture was mechanically stirred at 300 rpm in a nitrogen atmosphere, and the temperature was raised to 80°C. Then, 1 g of styrene, loaded in a micro-injector (model TJ-1A/L0107-1A, Longer), was injected slowly with a rate of 1 ml h^{-1} to the three-necked flask. Five hours after the addition of styrene, 0.5 g of photoinitiator (HMEM) in acetone (mass ratio of 1 : 5) was added to the system at a rate of 10 min ml^{-1} in the dark. After continuous reaction for 12 h, a thin layer of photoinitiator was coated on the magnetic polystyrene core. The magnetic nanospheres synthesized by seed emulsion polymerization are denoted as magnetic nanospheres coated by photoinitiator (MNS2).

## 2.5. Synthesis of poly(acrylic acid) coated magnetic nanospheres

MNS2 and AA monomer ($m_{MNS2} : m_{AA} = 1 : 1$) were added to a homemade photoreactor and the mixture was diluted to 1.0 wt% by deionized water. The reaction was started under UV lamp irradiation and completed in 2.5 h with vigorous magnetic stirring.

2.6. Characterization

The apparent hydrodynamic size and size distribution of the samples were obtained by dynamic light scattering (DLS) by NICOMP 380 ZLS measured at a fixed scattering angle of 90°. X-ray diffraction (XRD) analysis was performed with a Bruker D8 Advance X-ray diffractometer with a scan speed of 5° min^{-1} and an angular range of 10° to 90°. Thermogravimetric analysis (TGA) with a model Q600 SD was used to analyse the magnetite content at a heating rate of 10°C min^{-1} in air atmosphere. The hysteresis loop of the magnetic samples was characterized by a vibrating sample magnetometer (VSM, model Squid-VSM) with a test temperature of 298 K and a magnetic range of −20 kOe to 20 kOe. High-resolution transmission electron microscope (TEM) images were obtained at 200 kV using a JEOL-2100F.
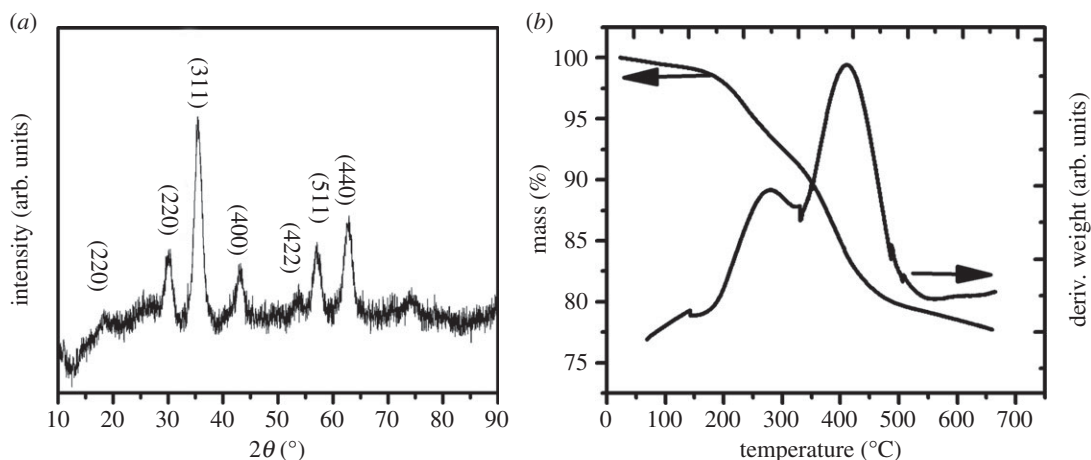
Figure 1. (*a*) XRD spectrum and (*b*) thermogravimetric analysis curve of MNP.
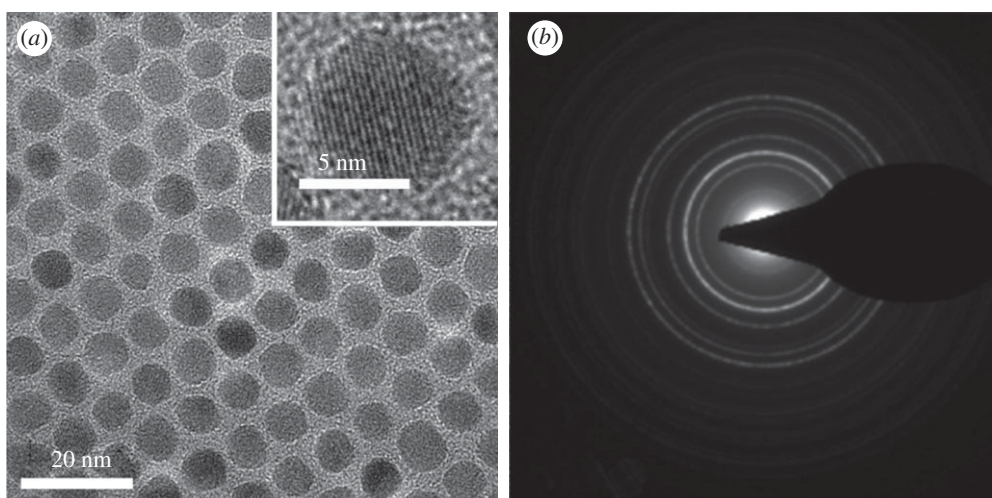
Figure 2. (*a*) TEM image and (*b*) selected area electron diffraction of MNP. Inset in (*a*) is a high-resolution image of a single MNP.

3. Results

3.1. Synthesis of magnetic nanospheres

3.1.1. Magnetic nanoparticles

In order to obtain MNP with uniform size and excellent magnetic properties, pyrolysis method was applied to synthesize oleic acid and oleylamine modified MNP. Excess oleic acid and oleylamine were used to obtain a highly stable magnetic fluid based on MNP. The structure of MNP was characterized by XRD as shown in figure 1*a*, and there are seven characteristic peaks at positions of 18.7° (220), 30.3° (220), 35.5° (311), 43.2° (400), 53.7° (422), 57.1° (511), 62.9° (440), which are consistent with the results reported in the literature [43,44]. The MNP size can be calculated by Scherrer formula based on XRD result and it is 8.9 nm [45]. TGA was employed to study the ligands (oleic acid and oleylamine) content on MNP surface and the result is shown in figure 1*b*. It was found that the total mass loss of oleic acid and oleylamine was 23% by weight, and there are two decomposition stages observed from the DTG curve in figure 1*b*. The corresponding decomposition temperatures are 257°C and 410°C, and the weight loss is 9% and 14%, respectively, indicating that there are two bonding ways of ligands on the surface of MNP. The weight loss at low temperature (110°C to 308°C) is caused by physical adsorption and the weight loss at high temperature (308°C to 530°C) is caused by chemical bonding [46,47].

TEM was used to observe the size and shape of the MNP as shown in figure 2. It showed that the diameter of the particles is about 9 nm, which is consistent with the calculated result from the XRD pattern in figure 1*a*. From the inset in figure 2*a*, a uniformly oriented lattice with explicit periphery
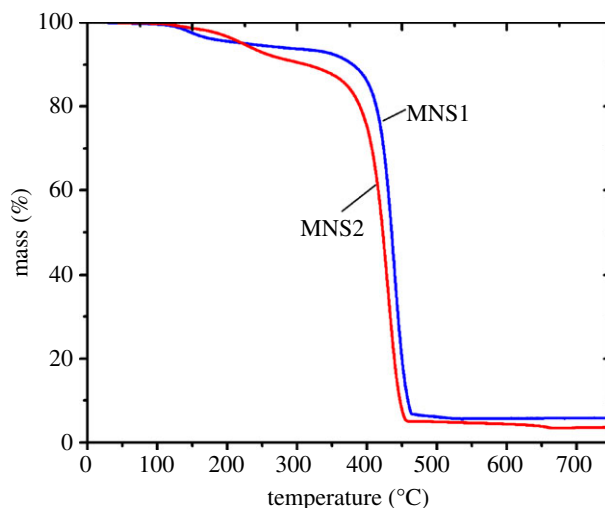
Figure 3. Thermogravimetric analysis curves of MNS1 and MNS2.

can be seen in a single MNP, indicating that each particle is a single crystal. The gap between each MNP is around 2 nm, which is ascribed to ligands (oleic acid and oleylamine) on MNP surface. Figure 2b shows the selected area electron diffraction mode obtained for 9 nm MNP, in line with the results of XRD.

3.1.2. Characterization of MNS1 and MNS2

Miniemulsion polymerization is known to be the best choice for encapsulating various types of nanoparticles, including MNP. But it was reported that MNP could move to the near surface of the nanosphere, which will influence further surface functionalization like immobilization of carboxyl groups [37]. Seed emulsion polymerization is known as an excellent tool to increase the seed size as well as redistribution of inorganic nanoparticles inside the seed [19]. It was reported that the particle morphology by seed emulsion polymerization was affected by the polymerization process [48]. There are two alternative processes, a swelling method and a semi-continuous feeding method. It is considered that monomer added by the swelling method initiates polymerization inside the seed, and the MNP would appear on the near surface or segregated on one side of the nanosphere due to the exclusion between different substances [41]. Compared to the swelling method, the semi-continuous feeding method is known to control the monomer feeding rate to reduce the matrix swelling to some extent and ensure the seed polymerization occurring on the seed surface [48]. Therefore, in order to reduce the adverse redistribution of MNP, the semi-continuous feeding method was chosen to add monomers during the seed emulsion polymerization process.

Figure 3 shows a TGA diagram of MNS1 and MNS2. The magnetite content is 5.9 wt% and 4.3 wt% for MNS1 and MNS2, respectively. Compared to MNS1, the decreased magnetite content of MNS2 is a result of increased content of polystyrene and photoinitiator HMEM. TEM is also used to characterize the change of size and morphology before and after seed emulsion polymerization. From the TEM images as shown in figure 4a,c, the size is ca 150 nm and 200 nm for MNS1 and MNS2, respectively, which is consistent with the data obtained from DLS measurements (figure 4b,d). More uniform nanospheres containing MNP could be seen in figure 4c and the polydispersity index of DLS also confirmed this finding (0.17 ± 0.02 for MNS1 and 0.11 ± 0.01 for MNS2). Averagely, the hydrodynamic size increased by 50 nm from MNS1 to MNS2. Both the decrease in MNP content and the increase in the diameter of the nanospheres confirmed the successful seed emulsion polymerization of MNS2 from MNS1.

3.1.3. Hysteresis loops

Magnetic properties of MNP, MNS1 and MNS2 at 298 K were recorded and compared using a VSM as shown in figure 5. In figure 5a, the saturation magnetizations of MNP, MNS1 and MNS2 are 52.4 emu g^{-1}, 2.7 emu g^{-1} and 0.96 emu g^{-1}, respectively. In figure 5b, the saturation magnetization value of MNP is 68.0 emu g^{-1} (ligands were subtracted according to TGA results). The inset in the upper left corner shows a small residual magnetization (0.75 emu g^{-1}) and coercive force (30 Oe), at which MNP are considered to be superparamagnetic [49]. In figure 5b, the saturation magnetizations of
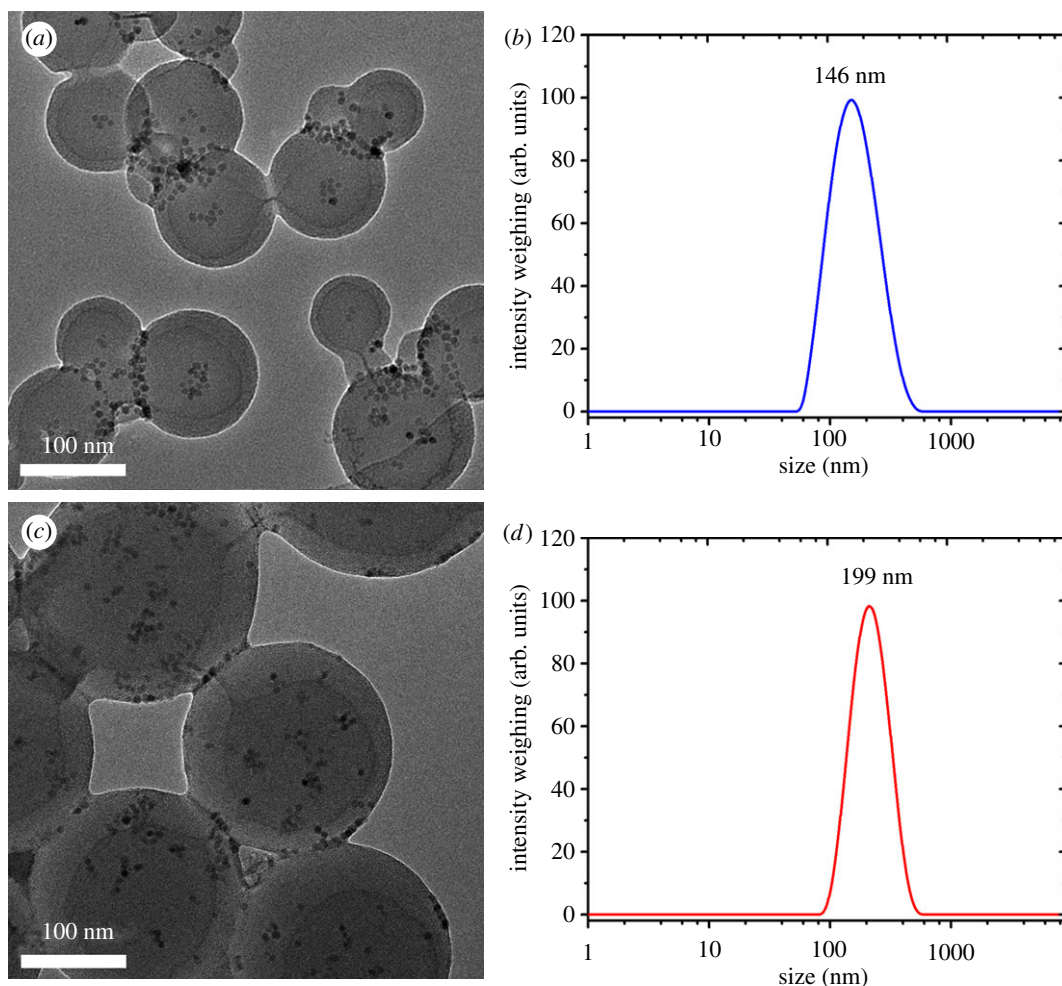
Figure 4. TEM images of (*a*) MNS1 and (*c*) MNS2, and hydrodynamic sizes of (*b*) MNS1 and (*d*) MNS2.
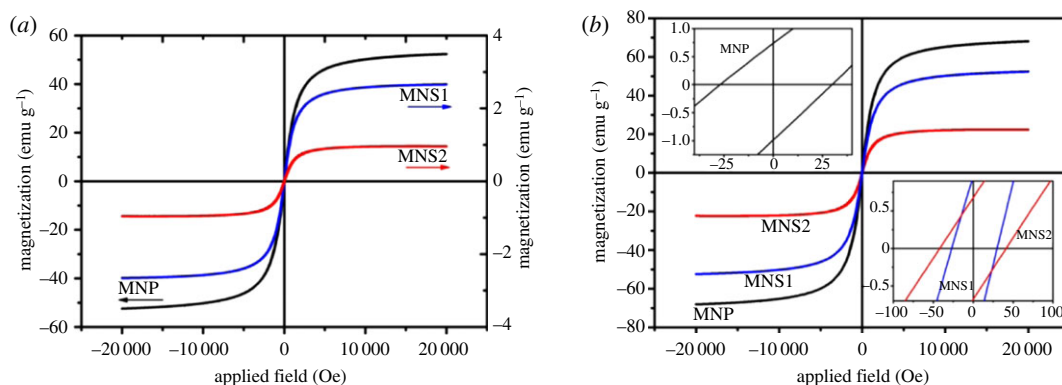
Figure 5. (*a*) Hysteresis loops and (*b*) hysteresis loops excluding the ligands and polymers of MNP, MNS1, and MNS2 at 298 K. The insets are enlarged plots.

MNS1 and MNS2 were reduced to 45.1 emu g^{-1} and 22.3 emu g^{-1} (ligands and polymer were subtracted according to TGA results), respectively. The residual magnetizations and coercive forces of MNS1 and MNS2 remain within the superparamagnetic range. Compared with MNP, the saturation magnetizations of MNS1 and MNS2 were reduced by 33.7% and 67.2%, respectively. After polymer encapsulation, the nanospheres still show superparamagnetism, but the saturation magnetization decreases as polymer content increases. The decrease in the saturation magnetization may be ascribed to the fact that the higher-powered ultrasonic operation causes partial oxidation of the magnetite nanoparticles to form non-magnetic iron oxide during the emulsifying process. In addition, the encapsulation of the polymer shell may also result in a loss of magnetization [50].
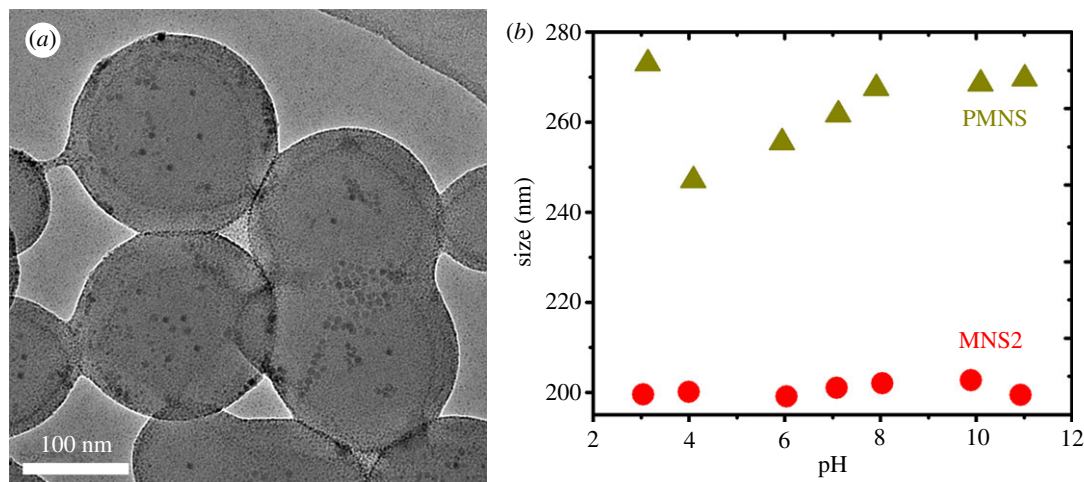
Figure 6. (*a*) TEM image of PMNS and (*b*) size of MNS2 and PMNS as a function of pH.

Table 1. Dosage and layer thickness in each step during the synthesis of PMNS.

| entry	styrene dosage (m_{St}/m_{MNS1})	L1 (nm)	AA dosage ($m_{AA} : m_{MNS2}$)	L2 (nm)	L (nm)
1	1.02	2.0	1 : 1	39.2	41.2
2	2.05	5.5	1 : 1	37.5	43.0
3	3.02	7.5	1 : 1	36.8	44.4
4	10.01	26.6	1 : 1	18.3	44.8

3.2. Synthesis of poly(acrylic acid) coated magnetic nanospheres

### 3.2.1. Poly(acrylic acid) grafting on MNS2

AA is chosen as a model functional monomer bearing negative carboxyl groups and was grafted on MNS2 surface by photoemulsion polymerization to obtain PMNS. Since the near surface of MNS2 is coated with a thin layer of photo-initiator HMEM, under the irradiation of ultraviolet light, AA is polymerized from the surface of MNS2 to form a brush-like PAA shell, which is reported in the literature as spherical PAA brushes [20]. In figure 6*a*, the size of diameter observed by TEM image changes little compared with that of MNS2 due to relatively low grafting density of PAA [51]. While, the successful PAA grafting can be characterized by DLS as shown in figure 6*b*. With the increase of pH value, the hydrodynamic size of MNS2 is almost a constant, because MNS2 has no pH sensitivity. As the pH increases, the thickness of the PAA layer increases, which is ascribed to deprotonation of carboxyl groups and electrostatic repulsion between negative charges. PMNS is unstable at low pH (pH $\leq$ 4) because of insufficient space hindrance and reduced electrostatic repulsion. The MNS2 showed a large amount of precipitation in one month. While the PMNS stored in a PBS buffer was stable for up to 6 months without precipitation, which demonstrated that the PAA chains endow PMNS with good stability. Compared to literature [52], however, the PAA length is relatively short under the same conditions. Considering that MNP may affect the photoinitiator encapsulation and then further PAA grafting, the relationship between shell increase in the MNS2 and PAA grafting in the PMNS will therefore be investigated.

3.2.2. Effect of seed emulsion polymerization on layer thickness of poly(acrylic acid) coated magnetic nanospheres

To reduce the MNP effect on further surface functionality of MNS2, styrene dosage was gradually increased as shown in table 1. The different particle size was calculated from DLS data and the corresponding sizes are illustrated in scheme 2. It was found that the size of polystyrene layer (L1) increased with the increase of
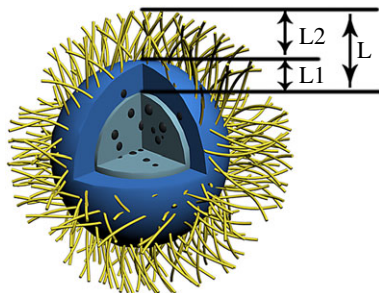
Scheme 2. Schematic illustration of different layers in the preparation process of PMNS. L1 means the increased size of polystyrene layer from MNS1. L2 means the increased size of PAA layer from MNS2. L means the combination of L1 and L2.
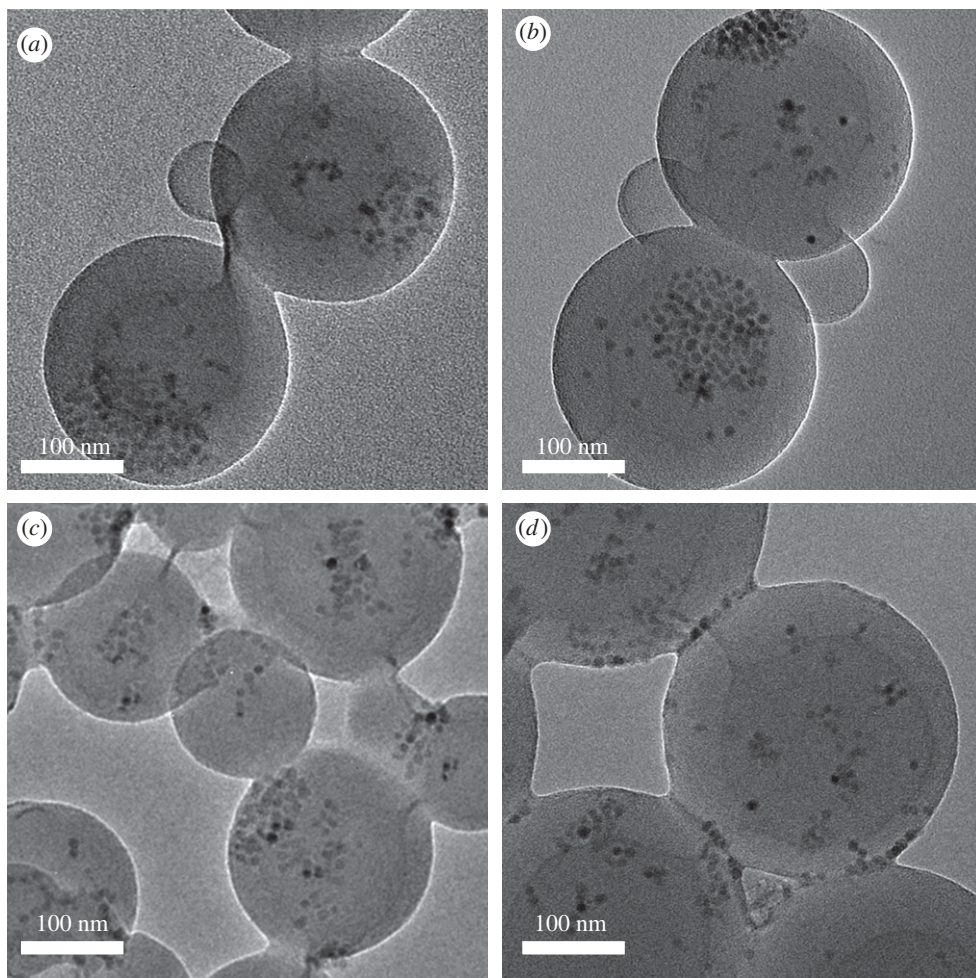
Figure 7. TEM images of (*a*) MNS1, (*b*) MNS2 of Entry 1, and (*c*) MNS1, (*d*) MNS2 of Entry 4.

styrene dosage, indicating more polymer was coated by seed emulsion polymerization mechanism. In the photoemulsion polymerization, the AA monomer dosage was kept as a constant ($m_{AA} : m_{MNS2} = 1 : 1$). It was surprising to find that the size of PAA layer (L2) decreased with the increase of styrene dosage in the seed emulsion polymerization. In order to figure out what happened during the multiple polymerization, TEM images of Entry 1 and Entry 4 were compared. For Entry 1 with a low styrene dosage, as shown in figure 7*a*,*b*, it was found that MNP appeared to be a cluster both in MNS1 and MNS2. But, for Entry 4 with a higher styrene dosage, MNP showed a more dispersed state inside MNS2 (figure 7*d*) compared to MNS1 (figure 7*c*). It indicates that excess styrene monomer may penetrate into the interior of MNS1 and initiate polymerization, resulting in a redistribution of MNP. Part of MNP would migrate to the near surface of MNS2, directly affecting the photoinitiator coating and further grafting efficiency of the PAA

on MNS2 surface. It is also found that the combined size ($L = 43 \pm 2$ nm) of L1 and L2 is approximately a constant for all entries in our experiments. Therefore, the total particle size is a balance between MNP distribution and PAA amount which was ascribed to the monomer penetration to nanospheres matrix when excess styrene monomer was added. Xu *et al.* used a seed emulsion polymerization method to increase the thickness of functional layer by approximately 10 nm [19]. Compared with the literature, our method improves the layer thickness to some extent.

4. Conclusion

PMNS containing MNP in the core and bearing PAA chains on the surface were prepared via a multiple polymerization route. MNP modified with oleic acid and oleylamine were synthesized by a pyrolysis route with a uniform size of 9 nm and ligand content of 23 wt%. The saturation magnetization of magnetite reached 68 emu g^{-1} and it is superparamagnetic. Seed emulsion polymerization by semi-continuous feeding method was successfully carried out on MNS1 to obtain MNS2. Both MNS1 and MNS2 showed superparamagnetic property but with decreased saturation magnetization by 33.7% and 67.2%. The pH sensitive PAA was finally grafted to MNS2 via photoemulsion polymerization. There was a balance between polystyrene layer thickness in MNS2 and PAA layer thickness in PMNS. Hence, we provide a novel multiple polymerization route to synthesize PMNS which would be very useful in a variety of areas like magnetic separation, biomedical field, etc.

References

1. Huang H, Kowalewski T, Wooley KL. 2003 Nanodroplets of polyisoprene fluid contained within poly(acrylic acid-co-acrylamide) shells. *J. Polym. Sci. A Polym. Chem.* **41**, 1659–1668. (doi:10.1002/pola.10712)

2. Blomberg S, Ostberg S, Harth E, Bosman AW, Van HB, Hawker CJ. 2002 Production of crosslinked, hollow nanoparticles by surface-initiated living free-radical polymerization. *J. Polym. Sci. A Polym. Chem.* **40**, 1309–1320. (doi:10.1002/pola.10210)

3. Du T, Ma S, Pei X, Wang S, Zhou F. 2017 Bio-inspired design and fabrication of micro/nano-brush dual structural surfaces for switchable oil adhesion and antifouling. *Small* **13**, 1602020. (doi:10.1002/smll.201602020)

4. Banerjee SS, Chen DH. 2007 Magnetic nanoparticles grafted with cyclodextrin for hydrophobic drug delivery. *Chem. Mater.* **19**, 6345–6349. (doi:10.1021/cm702278u)

5. Gupta AK, Curtis ASG. 2004 Surface modified superparamagnetic nanoparticles for drug delivery: interaction studies with human fibroblasts in culture. *J. Mater. Sci. Mater. Med.* **15**, 493–496. (doi:10.1023/B:JMSM. 0000021126.32934.20)

6. Yu H, Raymonda JW, Mcmahon TM, Campagnari AA. 2000 Detection of biological threat agents by immunomagnetic microsphere-based solid phase fluorogenic- and electro-chemiluminescence. *Biosens. Bioelectron.* **14**, 829–840. (doi:10.1016/S0956-5663(99)00068-8)

7. Li D, Tey WY, Cordelia S, Woodward RC, Rose A, Rosche B. 2007 Flame-sprayed superparamagnetic bare and silica-coated maghemite nanoparticles: synthesis, characterization, and protein adsorption-desorption. *Chem. Mater.* **18**, 6403–6413. (doi:10.1021/cm061861v)

8. Yang J et al. 2007 Synthesis of ultrasensitive magnetic resonance contrast agents for cancer imaging using PEG-fatty acid. *Chem. Mater.* **19**, 3870–3876. (doi:10.1021/cm070495s)

9. Halavaara J, Tervahartiala P, Isoniemi H, Höckerstedt K. 2015 Efficacy of sequential use of superparamagnetic iron oxide and gadolinium in liver MR imaging. *Acta Radiol.* **43**, 180–185. (doi:10.1080/028418502127347727)

10. Kawashita M, Tanaka M, Kokubo T, Inoue Y, Yao T, Hamada S, Shinjo T. 2005 Preparation of ferrimagnetic magnetite microspheres for in situ hyperthermic treatment of cancer. *Biomaterials* **26**, 2231–2238. (doi:10.1016/j.biomaterials. 2004.07.014)

11. Oster J, Parker J, Brassard LÀ. 2001 Polyvinyl-alcohol-based magnetic beads for rapid and efficient separation of specific or unspecific nucleic acid sequences. *J. Magn. Magn. Mater.* **225**, 145–150. (doi:10.1016/s0304-8853(00)01243-9)

12. Nishio K et al. 2008 Development of novel magnetic nano-carriers for high-performance affinity purification. *Colloids Surf. B Biointerfaces* **64**, 162–169. (doi:10.1016/j.colsurfb.2008. 01.013)

13. Zhang X, Tang X, Huang X. 2009 Synthesis of novel magnetic phosphazene-containing polymer microspheres with active hydroxyl groups. *J. Magn. Magn. Mater.* **321**, 2966–2970. (doi:10.1016/j.jmmm.2009.04.062)

14. Jiang H, Zhao L, Gai L, Wang Y, Hou Y, Liu H. 2015 Conjugation of methotrexate onto dedoped Fe$_3$O$_4$/PPy nanospheres to produce magnetic targeting drug with controlled drug release and targeting specificity for HeLa cells. *Synth. Met.* **207**, 18–25. (doi:10.1016/j. synthmet.2015.06.006)

15. Niu D, Li Y, Qiao X, Li L, Zhao W, Chen H, Zhao Q, Ma Z, Shi J. 2008 A facile approach to fabricate functionalized superparamagnetic copolymer-silica nanocomposite spheres. *Chem. Commun.* 4463–4465. (doi:10.1039/B807781A)

16. Ge Y, Zhang S, He S, Zhang Y, Gu N. 2009 Fabrication and characterization of chitosan-

poly(acrylic acid) magnetic nanospheres. *J. Nanosci. Nanotechnol.* **9**, 1287. (doi:10.1166/jnn.2009.C139)

17. Niu D *et al.* 2010 Preparation of uniform, water-soluble, and multifunctional nanocomposites with tunable sizes. *Adv. Funct. Mater.* **20**, 773–780. (doi:10.1002/adfm.200901493)

18. Bicak N, Gazi M, Galli G, Chiellini E. 2006 Polystyrene microspheres having epoxy functional dangling chains linked by hydrolytically stable bonds via ATRP. *J. Polym. Sci. A Polym. Chem.* **44**, 6708–6716. (doi:10.1002/pola.21756)

19. Xu Y, Xu H, Gu H. 2010 Controllable preparation of epoxy-functionalized magnetic polymer latexes with different morphologies by modified miniemulsion polymerization. *J. Polym. Sci. A Polym. Chem.* **48**, 2284–2293. (doi:10.1002/pola.23984)

20. Guo X, Weiss A, Ballauff M. 1999 Synthesis of spherical polyelectrolyte brushes by photoemulsion polymerization. *Macromolecules* **32**, 6043–6046. (doi:10.1021/ma990609o)

21. Fan W, Liu L, Zhao H. 2017 Co-assembly of patchy polymeric micelles and protein molecules. *Angew. Chem. Int. Ed.* **56**, 8844–8848. (doi:10.1002/anie.201704955)

22. Wang X, Shi Y, Graff RW, Lee D, Gao H. 2015 Developing recyclable pH-responsive magnetic nanoparticles for oil–water separation. *Polymer* **72**, 361–367. (doi:10.1016/j.polymer.2014.12.056)

23. Czeslik C, Jackler G, Hazlett T, Gratton E, Steitz R, Wittemann A, Ballauff M. 2004 Salt-induced protein resistance of polyelectrolyte brushes studied using fluorescence correlation spectroscopy and neutron reflectometry. *Phys. Chem. Chem. Phys.* **6**, 5557–5563. (doi:10.1039/b410805a)

24. Wittemann A, Haupt B, Ballauff M. 2003 Adsorption of proteins on spherical polyelectrolyte brushes in aqueous solution. *Phys. Chem. Chem. Phys.* **5**, 1671–1677. (doi:10.1039/B300607G)

25. Lu Y, Wittemann A, Ballauff M. 2010 Supramolecular structures generated by spherical polyelectrolyte brushes and their application in catalysis. *Macromol. Rapid Commun.* **30**, 806–815. (doi:10.1002/marc.200800789)

26. Schrinner M, Ballauff M, Talmon Y, Kauffmann Y, Thun J, Mller M, Breu J. 2009 Single nanocrystals of platinum prepared by partial dissolution of Au-Pt nanoalloys. *Science* **323**, 617–620. (doi:10.1126/science.1166703)

27. Lu Y, Mei Y, Schrinner M, Ballauff M, Moller WM, Breu J. 2007 In situ formation of Ag nanoparticles in spherical polyacrylic acid brushes by UV irradiation. *J. Phys. Chem. C* **111**, 7676–7681. (doi:10.1021/jp070973m)

28. Schrinner M, Proch S, Mei Y, Kempe R, Miyajima N, Ballauff M. 2010 Stable bimetallic gold–platinum nanoparticles immobilized on spherical polyelectrolyte brushes: synthesis, characterization, and application for the

oxidation of alcohols. *Adv. Mater.* **20**, 1928–1933. (doi:10.1002/adma.200702421)

29. Qiu GM, Zhu BK, Xu YY. 2005 α-Amylase immobilized by Fe₃O₄/poly(styrene-co-maleic anhydride) magnetic composite microspheres: preparation and characterization. *J. Appl. Polym. Sci.* **95**, 328–335. (doi:10.1002/app.21239)

30. Qiu GM, Xu YY, Zhu BK, Qiu GL. 2005 Novel, fluorescent, magnetic, polysaccharide-based microsphere for orientation, tracing, and anticoagulation: preparation and characterization. *Biomacromolecules* **6**, 1041–1047. (doi:10.1021/bm049302+)

31. Huang J, Wan S, Guo M, Yan H. 2006 Preparation of narrow or mono-disperse crosslinked poly((meth)acrylic acid)/iron oxide magnetic microspheres. *J. Mater. Chem.* **16**, 4535–4541. (doi:10.1039/b609088e)

32. Xu XL, Friedman G, Humfeld KD, Majetich SA, Asher SA. 2002 Synthesis and utilization of monodisperse superparamagnetic colloidal particles for magnetically controllable photonic crystals. *Chem. Mater.* **14**, 1249–1256. (doi:10.1021/cm010811h)

33. Liu X, Guan Y, Ma Z, Liu H. 2004 Surface modification and characterization of magnetic polymer nanospheres prepared by miniemulsion polymerization. *Langmuir* **20**, 10278–10282. (doi:10.1021/la0491908)

34. Landfester K. 2001 The generation of nanoparticles in miniemulsions. *Adv. Mater.* **13**, 765–768. (doi:10.1002/1521-4095(200105)13:10<765::AIDADMA765>3.0.CO;2-F)

35. Ramírez LP, Landfester K. 2003 Magnetic polystyrene nanoparticles with a high magnetite content obtained by miniemulsion processes. *Macromol. Chem. Phys.* **204**, 22–31. (doi:10.1002/macp.200290052)

36. Csetneki I, Faix MK, Szilágyi A, Kovács AL, Németh Z, Zrinyi M. 2004 Preparation of magnetic polystyrene latex via the miniemulsion polymerization technique. *J. Polym. Sci. A Polym. Chem.* **42**, 4802–4808. (doi:10.1002/pola.20300)

37. Chen K, Zhu Y, Zhang Y, Li L, Lu Y, Guo X. 2011 Synthesis of magnetic spherical polyelectrolyte brushes. *Macromolecules* **44**, 632–639. (doi:10.1021/ma102337c)

38. Wang PC, Chiu WY, Lee CF, Young TH. 2004 Synthesis of iron oxide/poly(methyl methacrylate) composite latex particles: nucleation mechanism and morphology. *J. Polym. Sci. A Polym. Chem.* **42**, 5695–5705. (doi:10.1002/pola.20335)

39. Chen T, Wang L, Jiang G, Wang J, Wang J, Zhou J. 2005 Poly(ferrocenyldimethylsilane-b-dimethylsiloxane) microsphere with shell thickness controllable structure prepared through self-assembly. *Polymer* **46**, 5773–5777. (doi:10.1016/j.polymer.2005.05.049)

40. Wen D, Zeng HM, Wang YY, Lai QY, Ji XY, WenD ZH, Wang Y Y, Lai QY, Ji XY. 2008 Self-assembling magnetic microspheres by P(St-co-AA) and Fe₃O₄ nanoparticles. *J. Inorg.*

Mater. **23**, 29–32. (doi:10.3724/SP.J.1077.2008.00029)

41. Yu X, Huang S, Chen K, Zhou Z, Guo X, Li L. 2015 Preparation of functional Janus particles with response to magnetic force. *Ind. Eng. Chem. Res.* **54**, 2690–2696. (doi:10.1021/ie504299t)

42. Sun S, Zeng H, Robinson DB, Raoux S, Rice PM, Wang SX, Li G. 2004 Monodisperse MFe₂O₄ (M = Fe, Co, Mn) nanoparticles. *J. Am. Chem. Soc.* **126**, 273–279. (doi:10.1021/ja0380852)

43. Gong T, Yang D, Hu J, Yang W, Wang C, Lu JQ. 2009 Preparation of monodispersed hybrid nanospheres with high magnetite content from uniform Fe₃O₄ clusters. *Colloids Surf. A Physicochem. Eng. Asp.* **339**, 232–239. (doi:10.1016/j.colsurfa.2009.02.034)

44. Patterson AL. 1939 The Scherrer formula for X-ray particle size determination. *Phys. Rev.* **56**, 978–982. (doi:10.1103/PhysRev.56.978)

45. Montagne F, Mondain-Monval O, Pichot C, Mozzanega H, ElaïSsari A. 2002 Preparation and characterization of narrow sized (o/w) magnetic emulsion. *J. Magn. Magn. Mater.* **250**, 302–312. (doi:10.1016/s0304-8853(02)00412-2)

46. Klug HP, Alexander LE. 1974 *X-ray diffraction procedures: for polycrystalline and amorphous materials*, 2nd edn. Weinheim, Germany: Wiley-VCH.

47. Min TI, Klein A, El-Aasser MS, Vanderhoff JW. 1983 Morphology and grafting in polybutylacrylate-polystyrene core-shell emulsion polymerization. *J. Polym. Sci. A Polym. Chem.* **21**, 2845–2861. (doi:10.1002/pol.1983.170211001)

48. Li L, Yang Y, Ding J, Xue J. 2010 Synthesis of magnetite nanooctahedra and their magnetic field-induced two-/three-dimensional superstructure. *Chem. Mater.* **22**, 3183–3191. (doi:10.1021/cm100289d)

49. Hong RY, Feng B, Liu G, Wang S, Li HZ, Ding JM, Zheng Y, Wei DG. 2009 Preparation and characterization of Fe₃O₄/polystyrene composite particles via inverse emulsion polymerization. *J. Alloys Compd.* **476**, 612–618. (doi:10.1016/j.jallcom.2008.09.060)

50. Wittemann A, Drechsler M, Talmon Y, Ballauff M. 2005 High elongation of polyelectrolyte chains in the osmotic limit of spherical polyelectrolyte brushes: a study by cryogenic transmission electron microscopy. *J. Am. Chem. Soc.* **127**, 9688–9689. (doi:10.1021/ja0513234)

51. Chen K, Zhu Y, Li L, Yan LY, Guo X. 2010 Recyclable spherical polyelectrolyte brushes containing magnetic nanoparticles in core. *Macromol. Rapid Commun.* **31**, 1440–1443. (doi:10.1002/marc.201000195)

52. Niu D *et al.* 2011 Fabrication of uniform, biocompatible and multifunctional PCL-b-PAA copolymer-based hybrid micelles for magnetic resonance imaging. *J. Mater. Chem.* **21**, 13825–13831. (doi:10.1039/c1jm10929d)